Draft version February 5, 2008
Preprint typeset using LaTeX style emulateapj v. 14/09/00

CONSTRAINTS ON Ω_M AND σ_8 FROM WEAK LENSING IN RCS FIELDS

Henk Hoekstra[1,2,3], H.K.C. Yee[2,3,4], and Michael D. Gladders[2,3,4,5]

Draft version February 5, 2008

ABSTRACT

We have analysed 53 square degrees of R_C-band imaging data from the Red-Sequence Cluster Survey (RCS), and measured the excess correlations in the shapes of galaxies on scales out to ~ 1.5 degrees. We separate the signal into an "E"- (lensing) and "B"-mode (systematics), which allows us to study the contribution from residual systematics and intrinsic alignments. On scales larger than 10 arcminutes, we find no "B"-mode, suggesting that the signal at those scales is solely caused by gravitational lensing. On smaller scales we find a small, but significant "B"-mode. This signal is also present when we select a sample of bright ($20 < R_C < 22$) galaxies. These galaxies are rather insensitive to observational distortions, and we therefore conclude that the observed "B"-mode is likely to be caused by intrinsic alignments. To minimize the effect of intrinsic alignments, we limit the cosmic shear analysis to galaxies with $22 < R_C < 24$.

We derive joint constraints on Ω_m and σ_8, by marginalizing over Γ, Ω_Λ and the source redshift distribution, using different priors. Marginalizing over Γ and Ω_Λ, and using a flat prior for the source redshift distribution, yields a conservative constraint of $\sigma_8 = 0.45^{+0.09}_{-0.12}\Omega_m^{-0.55}$ (95% confidence). A better constraint is derived when we use Gaussian priors for Γ (from the 2dF survey) and $\Omega_m + \Omega_\Lambda$ (from CMB), and the source redshift distribution. For this choice of priors, we find $\sigma_8 = (0.46^{+0.05}_{-0.07})\Omega_m^{-0.52}$ (95% confidence). We also investigated whether the RCS data can be used to constrain Γ. Using our set of Gaussian priors, we find that we can only place a lower bound on Γ for which we find $\Gamma > 0.1 + 0.16\Omega_m$ (95% confidence).

Comparison of the RCS results with three other recent cosmic shear measurements shows excellent agreement. The current weak lensing results are also in good agreement with CMB measurements, when we allow the reionization optical depth τ and the spectral index n_s to vary. We present a simple demonstration of how the weak lensing results can be used as a prior in the parameter estimation from CMB measurements to derive constraints on the reionization optical depth τ.

Subject headings: cosmology: observations − dark matter − gravitational lensing

1. INTRODUCTION

The measurement of the coherent distortions of the images of faint galaxies caused by weak lensing by intervening large scale structures provides a direct way to study the statistical properties of the growth of structures in the universe. Compared to many other methods, such as redshift surveys (e.g., Strauss & Willick 1995; Peacock et al. 2001; Percival et al. 2001), weak lensing probes the dark matter distribution directly, regardless of the light distribution. In addition, it provides measurements on scales from the quasi-linear to the non-linear regime, where comparisons between observations and predictions are still limited.

The distortion in the images of distant galaxies is small, and consequently it is not measured easily. Only recently it has become possible to measure the signal and the number of published measurements is increasing rapidly (e.g., Bacon et al. 2000, 2002; Hoekstra et al. 2002a; Kaiser, Wilson, & Luppino 2000; Maoli et al. 2000; Refregier, Rhodes, & Groth 2002; van Waerbeke 2000, 2001a, 2002; Wittman et al. 2000).

Weak lensing observations can be used for a wide range of studies. For instance, Hoekstra, Yee, & Gladders (2001) presented a first measurement of a combination of the bias parameter and the galaxy-mass cross-correlation coefficient as a function of scale. The first direct measurement of the bias parameter and the galaxy-mass cross-correlation coefficient was presented by Hoekstra et al. (2002b). These studies provide unique constraints on models of galaxy formation. Another important application is to constrain cosmological parameters from the measurement of the two-point statistics of the dark matter distribution.

The amplitude of the lensing signal depends on many parameters, of which some are degenerate. Some of the degeneracies can be overcome using measurements that probe the dark matter power spectrum at different redshifts, or by comparison of the results in the linear regime to the non-linear scales. Such subtle differences require very accurate measurements, which are currently not available. Planned large surveys, such as the CFHT Legacy Survey, however, will be a major advance in this area. Also higher order statistics, such as the skewness, are po-

[1] CITA, University of Toronto, Toronto, Ontario M5S 3H8, Canada
[2] Department of Astronomy, University of Toronto, Toronto, Ontario M5S 3H8, Canada
[3] Visiting Astronomer, Canada-France-Hawaii Telescope, which is operated by the National Research Council of Canada, Le Centre National de Recherche Scientifique, and the University of Hawaii
[4] Guest observer at the Cerro Tololo Inter-American Observatory (CTIO), a division of the National Optical Astronomy Observatories, which is operated by the Association of Universities for Research in Astronomy, Inc., under cooperative agreement with the National Science Foundation
[5] Observatories of the Carnegie Institution of Washington, 813 Santa Barbara Street, Pasadena, California 91101

tentially powerful tools to break some of the degeneracies (e.g., Schneider et al. 1998).

Better constraints can be obtained by combining the weak lensing measurements with results from other techniques. In particular the combination with cosmic microwave background (CMB) measurements is useful, because the physics of both lensing and CMB are well understood. Also some results from galaxy redshift surveys can be used, provided they are made in the linear regime, and under the assumption that the bias is constant with scale.

In this paper we present the results from our analysis of ~ 53 deg^2 of R_C-band data from the Red-Sequence Cluster Sequence (RCS) (e.g., Yee & Gladders 2001), which is a 90 deg^2 galaxy cluster survey designed to provide a large sample of optically selected clusters of galaxies with redshifts $0.1 < z < 1.4$.

Hoekstra et al. (2002a) used a subset of the current data to study the cosmic shear. Compared to other cosmic shear studies, the RCS data are shallow, and consequently the signal at a given scale is much lower, as is the signal-to-noise ratio. However, measuring the weak lensing signal from a shallow survey has several advantages. Down to a limiting magnitude of $R_C \sim 24$ star-galaxy separation works well (see Fig. 1 from Hoekstra et al 2002a). In deeper surveys many sources have sizes comparable to the size of the PSF, and applying size cuts may change the redshift distribution of the sources in a systematic way. In addition, down to $R_C \sim 24$ the redshift distribution of the sources is fairly well determined. In order to relate the observed cosmic shear signal to cosmological parameters, a good understanding of the source redshift distribution is crucial.

One worry is the effect of intrinsic alignments of the source galaxies, which introduces an additional signal (e.g., Heavens et al. 2000; Catelan et al. 2001; Crittenden et al. 2001; Mackey et al. 2001). The amplitude of the effect is not well determined, but it is clear that it is more important for shallower surveys. However, the predictions indicate that for a median redshift of $z = 0.6$ (which is similar to our sample of source galaxies) the signal caused by intrinsic alignments is still small compared to the lensing signal.

The structure of the paper is as follows. In §2 we briefly discuss the theory of lensing by large scale structure. The data and measurements are presented in §3. We compare the measurements to model predictions in a maximum likelihood analysis in §4. We summarize our results in §5.

2. METHOD

In this section we provide a basic description of the theory of weak lensing by large scale structure. We discuss the dependence on the assumed cosmology and the redshifts of the sources. Detailed discussions on this subject can be found elsewhere (e.g., Schneider et al. 1998; Bartelmann & Schneider 2001).

The observable two-point statistics can be related to the convergence power spectrum, which is defined as

$$P_\kappa(l) = \frac{9H_0^4\Omega_m^2}{4c^4} \int_0^{w_H} dw \left(\frac{\bar{W}(w)}{a(w)}\right)^2 P_\delta\left(\frac{l}{f_K(w)}; w\right), \quad (1)$$

where w is the radial (comoving) coordinate, w_H corresponds to the horizon, $a(w)$ the cosmic scale factor, and $f_K(w)$ the comoving angular diameter distance. As shown by Jain & Seljak (1997) and Schneider et al. (1998) it is necessary to use the non-linear power spectrum in equation (1). This power spectrum is derived from the linear power spectrum following the prescriptions from Peacock & Dodds (1996).

$\bar{W}(w)$ is the source-averaged ratio of angular diameter distances D_{ls}/D_s for a redshift distribution of sources $p_b(w)$:

$$\bar{W}(w) = \int_w^{w_H} dw' p_b(w') \frac{f_K(w'-w)}{f_K(w')}. \quad (2)$$

Hence, it is important to know the redshift distribution of the sources, in order to relate the observed lensing signal to $P_\kappa(l)$.

In Hoekstra et al. (2002a) we used the top-hat smoothed variance as a measure of the cosmic shear signal. The top-hat variance $\langle\gamma^2\rangle$ is related to the convergence power spectrum through

$$\langle\gamma^2\rangle(\theta) = 2\pi \int_0^\infty dl\ l\ P_\kappa(l) \left[\frac{J_1(l\theta)}{\pi l\theta}\right]^2, \quad (3)$$

where θ is the radius of the aperture used to compute the variance, and J_1 is the first Bessel function of the first kind. Hoekstra et al. (2002a) measured the top-hat variance by actually computing the excess variance in apertures.

Recent studies, however, show that an optimal use of the data is to measure the shear correlation functions from the data directly. These correlation functions can be related to the various two-point statistics. In addition, this approach allows one to split the signal into two components: an "E"-mode, which is curl-free, and a "B"-mode, which is sensitive to the curl of the shear field. Gravitational lensing arises from a gravitational potential, and hence it is expected to produce a curl-free shear field. Hence, the "B"-mode can be used to quantify the level of systematics involved in the measurement.

Several sources of "B"-mode have been identified. Schneider et al. (2002) showed how redshift clustering of source galaxies can introduce a "B"-mode. However, in most situations the contribution to the observed signal is negligible. Simple models describing the intrinsic alignments of galaxies predict a small "B"-mode (Crittenden et al. 2002), although the amplitude is still uncertain. Hence, any measured "B"-mode is dominated by residual systematics in the data (e.g., imperfect correction of the PSF anisotropy) or intrinsic alignments. The effect of intrinsic alignments can be minimized by selecting galaxies with a broad redshift distribution. In future surveys, with photometric redshift information for the galaxies, the contribution from intrinsic alignments can be removed completely by correlating the shapes of galaxies with different redshifts.

The decompositions of the shear correlation function and the top-hat variance in E and B modes are defined up to a constant (Crittenden et al. 2002; Pen et al. 2002). The decomposition is naturally carried out by using the aperture mass statistic $M_{\rm ap}$. Kaiser et al. (1994) introduced this statistic to measure the masses of clusters of

galaxies. Its usefulness for the study of cosmic shear was pointed out by Schneider et al. (1998). The aperture mass is defined as

$$M_{\rm ap}(\theta) = \int d^2\phi U(\phi)\kappa(\phi). \quad (4)$$

Provided $U(\phi)$ is a compensated filter, i.e., $\int d\phi\phi U(\phi) = 0$, with $U(\phi) = 0$ for $\phi > \theta$, the aperture mass can be expressed in term of the observable tangential shear $\gamma_{\rm t}$ using a different filter function $Q(\phi)$ (which is a function of $U(\phi)$),

$$M_{\rm ap}(\theta) = \int_0^\theta d^2\phi Q(\phi)\gamma_{\rm t}(\phi). \quad (5)$$

We use the filter function suggested by Schneider et al. (1998)

$$U(\theta) = \frac{9}{\pi\theta^2}\left(1-\frac{\vartheta^2}{\theta^2}\right)\left(\frac{1}{3}-\frac{\vartheta^2}{\theta^2}\right), \quad (6)$$

for $\theta \leq \vartheta$, and 0 elsewhere. The corresponding $Q(\theta)$ is given by

$$Q(\theta) = \frac{6}{\pi\theta^2}\left(\frac{\vartheta^2}{\theta^2}\right)\left(1-\frac{\vartheta^2}{\theta^2}\right), \quad (7)$$

for $\theta \leq \vartheta$, and 0 elsewhere. With this choice of filter functions, the variance of the aperture mass $\langle M_{\rm ap}^2\rangle$ is related to the power spectrum through

$$\langle M_{\rm ap}^2\rangle = 2\pi\int_0^\infty dl\ lP_\kappa(l)\left[\frac{12}{\pi(l\theta)^2}J_4(l\theta)\right]^2, \quad (8)$$

where J_4 is the fourth-order Bessel function of the first kind.

A straightforward implementation of the aperture mass statistic is to compute $M_{\rm ap}$ directly from the data using the estimator (e.g., Schneider et al. 1998)

$$\tilde{M}_{\rm ap} = \pi\theta^2\frac{\sum_{i=1}^{N_s} Q(\theta_i)w_i\gamma_{{\rm t},i}}{\sum_{i=1}^{N_s} w_i}, \quad (9)$$

where N_s is the number of source galaxies, $\gamma_{{\rm t},i}$ is the tangential shear of the ith galaxy with respect to the center of the aperture. The weights w_i correspond to the inverse square of the uncertainty in the shape measurement (Hoekstra et al. 2000).

One can use this procedure to tile the observed fields with apertures, and compute the excess variance. However, this approach assumes that the data are contiguous, which is not the case for real data. The masking of the RCS data is not severe, but does complicate a measurement of $\langle M_{\rm ap}^2\rangle$ through this method.

Instead, we will determine $\langle M_{\rm ap}^2\rangle$ from the observed ellipticity correlation functions. This method has the advantage that it uses all information contained in the data, and that it does not depend on the geometry of the survey. Pen et al. (2002) were the first to apply this approach, using data from the VIRMOS-DESCART survey.

The two ellipticity correlation function that are measured are

$$\xi_{\rm tt}(\theta) = \frac{\sum_{i,j}^{N_s} w_iw_j\gamma_{{\rm t},i}(\mathbf{x}_i)\cdot\gamma_{{\rm t},j}(\mathbf{x}_j)}{\sum_{i,j}^{N_s} w_iw_j}, \quad (10)$$

and

$$\xi_{\rm rr}(\theta) = \frac{\sum_{i,j}^{N_s} w_iw_j\gamma_{{\rm r},i}(\mathbf{x}_i)\cdot\gamma_{{\rm r},j}(\mathbf{x}_j)}{\sum_{i,j}^{N_s} w_iw_j}, \quad (11)$$

where $\theta = |\mathbf{x}_i - \mathbf{x}_j|$. $\gamma_{\rm t}$ and $\gamma_{\rm r}$ are the tangential and 45 degree rotated shear in the frame defined by the line connecting the pair of galaxies. For the following, it is more useful to consider

$$\xi_+(\theta) = \xi_{\rm tt}(\theta) + \xi_{\rm rr}(\theta), \text{ and } \xi_-(\theta) = \xi_{\rm tt}(\theta) - \xi_{\rm rr}(\theta), \quad (12)$$

i.e., the sum and the difference of the two observed correlation functions. As shown by Crittenden et al. (2002), one can derive "E" and "B"-mode correlation functions by integrating $\xi_+(\theta)$ and $\xi_-(\theta)$ with an appropriate window function (see Pen et al. 2002 for an application to the VIRMOS-DESCART data).

The "E" and "B"-mode aperture masses are computed from the ellipticity correlation functions using

$$\langle M_{\rm ap}^2\rangle(\theta) = \int d\vartheta\ \vartheta\left[\mathcal{W}(\vartheta)\xi_+(\vartheta) + \tilde{\mathcal{W}}(\vartheta)\xi_-(\vartheta)\right], \quad (13)$$

and

$$\langle M_\perp^2\rangle(\theta) = \int d\vartheta\ \vartheta\left[\mathcal{W}(\vartheta)\xi_+(\vartheta) - \tilde{\mathcal{W}}(\vartheta)\xi_-(\vartheta)\right], \quad (14)$$

where $\mathcal{W}(\vartheta)$, and $\tilde{\mathcal{W}}(\vartheta)$ are given in Crittenden et al. (2002). Useful analytic expressions were derived by Schneider et al. (2001). Both $\mathcal{W}(\vartheta)$, and $\tilde{\mathcal{W}}(\vartheta)$ vanish for $\vartheta > 2\theta$, so that $\langle M_{\rm ap}^2\rangle$ can be obtained directly from the observable ellipticity correlation functions over a finite interval.

3. MEASUREMENTS

We use the R_C-band imaging data from the Red-Sequence Cluster Survey (RCS, Gladders & Yee 2000). The final survey covers 90 deg^2 in both R_C and z', spread over 22 widely separated patches of $\sim 2.1 \times 2.3$ degrees. The northern half of the survey was observed using the CFH12k camera on the CFHT, and the data from the southern half were obtained using the Mosaic II camera on the CTIO 4m telescope.

The integration times are 900s for the CFHT data and 1200s for the CTIO data. A subset of this data set was studied in Hoekstra et al. (2002a): 16.4 deg^2 CFHT data and 7.6 deg^2 of CTIO data. We augment the data used by Hoekstra et al. (2002a) by the remaining CFHT12k data. Much of the remaining CTIO data has relatively poor seeing, and hence is less useful for our weak lensing analysis and is not used. The seeing for the data used here ranges from $0\farcs57$ to $1\farcs39$ (only 11% of the data had seeing $> 1''$), with a median value of $0\farcs8$. Hence, the final data set studied here consists of a total of 53 deg^2 of imaging data, spread over 13 patches.

A detailed description of the data reduction and object analysis is described in Hoekstra et al. (2002a), to which we refer for technical details. Here we present a short description of the various steps in the analysis.

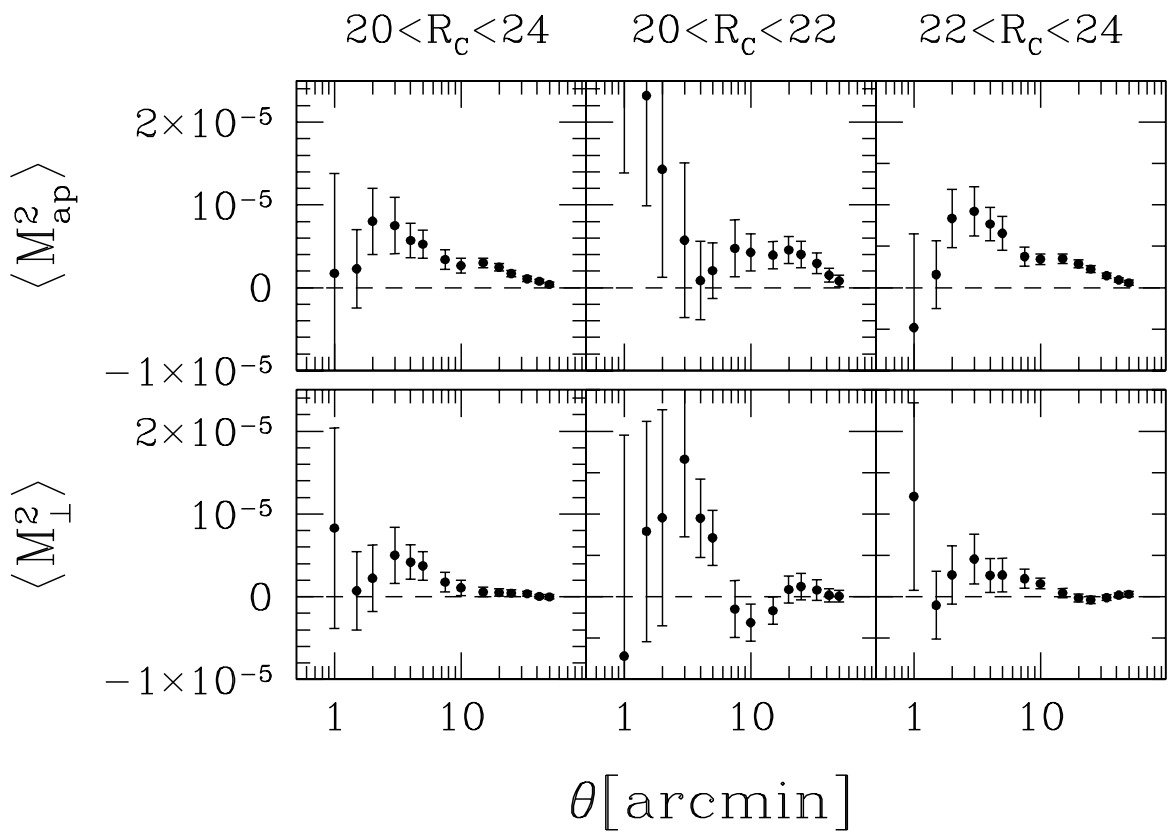

FIG. 1.— The upper panels show the measured variance of the aperture mass $\langle M_{\rm ap}^2 \rangle$ as a function of aperture size θ for different samples of source galaxies. This signal corresponds to the "E'-mode. The lower panels show the variance $\langle M_\perp^2 \rangle$ when the phase of the shear is increased by $\pi/2$, and corresponds to the "B"-mode. The error bars indicate the 1σ statistical uncertainty in the measurements, and have been derived from the field-to-field variation of the 13 patches (thus the error bars include cosmic variance). Note that the points are slightly correlated. We detect a significant "B"-mode on scales $5-10$ arcminutes. On scales larger than 10 arcminutes the "B"-mode vanishes. The sample of bright galaxies ($20 < R_C < 22$) should not be affected significantly by systematics because their sizes are large compared to the PSF. Therefore the significant "B"-mode at scales of a few arcminutes is likely to be caused by intrinsic alingments. To minimize the effect of intrinsic alignments on our cosmological parameter estimation, we will use the sample of galaxies with $22 < R_C < 24$ to this end.

We use single exposures in our analysis, and consequently cosmic rays have not been removed. However, cosmic rays are readily eliminated from the photometric catalogs: small, but very significant objects are likely to be cosmic rays, or artifact from the CCD. The peak finder gives fair estimates of the object size, and we remove all objects smaller than the size of the PSF.

The objects in this cleaned catalog are then analysed, which yield estimates for the size, apparent magnitude, and shape parameters (polarization and polarizabilities). The objects in this catalog are inspected by eye, in order to remove spurious detections. These objects have to be removed because their shape measurements are affected by cosmetic defects (such as dead columns, bleeding stars, halos, diffraction spikes) or because the objects are likely to be part of a resolved galaxy (e.g., HII regions).

To measure the small, lensing induced distortions in the images of the faint galaxies it is important to accurately correct the shapes for observational effects, such as PSF anisotropy, seeing and camera shear; PSF anisotropy can mimic a cosmic shear signal, and a correction for the seeing is required to relate the measured shapes to the real lensing signal. To do so, we follow the procedure outlined in Hoekstra et al. (1998). We select a sample of moderately bright stars from our observations, and use these to characterize the PSF anisotropy and seeing. We fit a second order polynomial to the shape parameters of the selected stars for each chip. These results are used to correct the shapes of the galaxies for PSF anisotropy and seeing.

The effect of the PSF is not the only observational distortion that has to be corrected. The optics of the camera stretches the images of galaxies (i.e., it introduces a shear) because of the non-linear remapping of the sky onto the CCD. We have used observations of astrometric fields to find the mapping between the sky and the CCD pixel coordinate system, and derived the corresponding camera shear, which is subsequently subtracted from the galaxy ellipticity (see Hoekstra et al. 1998).

As discussed in Hoekstra et al. (2002a) we use galaxies with $20 < R_C < 24$ in our analysis. This selection yields a sample of 1,773,543 galaxies for which we could determine useful shape parameters. We note that the sample is not complete at the faint limit.

The upper panels in Figure 1 show the measured vari-

ance of the aperture mass $\langle M_{\rm ap}^2 \rangle$ as a function of aperture size θ. For all three samples we find that the "B"-mode (lower panels) vanishes on scales larger than $\sim$ 10 arcminutes, suggesting that neither observational distortions or intrinsic alignments of sources have corrupted our measurements. This is quite different from the VIRMOS-DESCART results presented by Van Waerbeke et al. (2002) who found an almost constant "B"-mode out to scales of 30 arcminutes.

To study possible residual systematics introduced by the correction for the PSF and camera shear, we split the data into various subsets: good/bad seeing, small/large PSF anisotropy, center/edge of chip. In all three cases, we find excellent agreement between the subsets.

On smaller scales we detect a significant "B" mode. Interestingly, we detect also a significant signal for the bright galaxies ($20 < R_C < 22$). These galaxies have sizes that are large compared to the PSF, and therefore they are less affected by residual systematics, whereas intrinsic alignments are expected to be particularly important for bright galaxies. The selection of relatively bright galaxies in the R_C band results in a relatively narrow range in redshift as one essentially observes intrinsically fainter galaxies at redshifts $z = 0.3 - 0.5$. Only for fainter magnitude limits one overcomes the 4000Å break, and more distant galaxies enter in the sample. Hence, the "B"-mode at a few arcminutes is likely to be caused by intrinsic alignments.

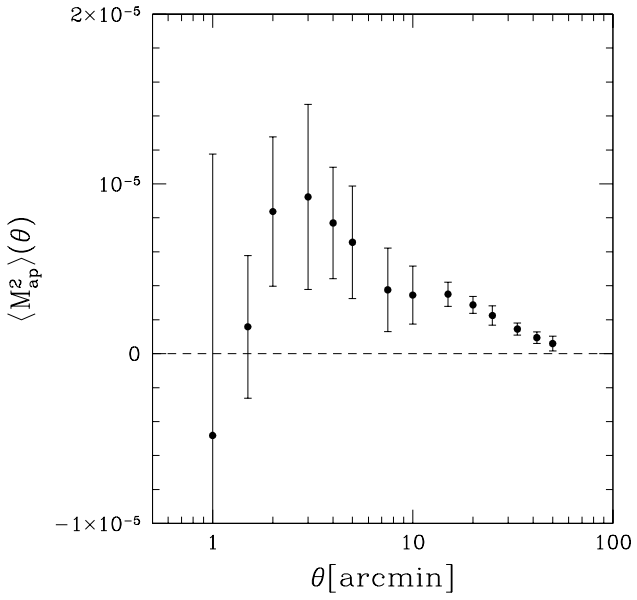

FIG. 2.— The measured variance of the aperture mass $\langle M_{\rm ap}^2 \rangle$ as a function of aperture size θ for source galaxies with $22 < R_C < 24$. The error bars have been increased to account for the unknown correction for the "B"-mode observed in Figure 1.

The full sample ($20 < R_C < 24$) includes the bright galaxies, and hence the contribution of intrinsic alignments to the signal is larger compared to the faint ($22 < R_C < 24$) sample. The fainter galaxies yield a slightly higher lensing signal, because the average redshift of the sources is higher. In addition the redshift distribution of galaxies with $22 < R_C < 24$ is also broader (see, e.g., Hoekstra 2001), which reduces the effect of intrinsic alignments.

Currently it is not clear how to correct the "E"-mode, given the observed "B"-mode. We follow Van Waerbeke et al (2002) and add the "B"-mode in quadrature to the uncertainty in the "E"-mode, as this provides a conservative limit to how well we can determine the lensing signal. The best signal-to-noise is obtained for the faint sample, and we will use this sample below for the cosmological parameter estimation.

Figure 2 shows the resulting measurement of $\langle M_{\rm ap}^2 \rangle$ as a function of scale when the error bars are increased using the observed "B"-mode.

4. CONSTRAINTS ON COSMOLOGICAL PARAMETERS

4.1. *Source redshift distribution*

We now need to relate the observed lensing signal, presented in Figure 2, to the cosmological parameters. To do so, we compute model predictions for a range of parameters using Eq. (8). However, the evaluation of Eq. (8) requires knowledge of the redshift distribution of the sources.

Compared to other, deeper, cosmic shear studies, the RCS data have the major advantage that the redshift distribution of the galaxies is known fairly well. Cohen et al. (2000) have determined spectroscopically the redshift distribution of galaxies down to a limiting magnitude of $R_C = 24$. However, their result is likely to suffer from sample variance. Comparison of the Cohen et al. (2000) redshifts with photometric redshifts (e.g., Fernández-Soto et al. 1999) showed that the latter provide a suitable way to derive the redshift distribution of the sources we consider here.

To do so, we have to account for the fact that the uncertainty in the shape measurements depend on the apparent magnitudes (and thus on the redshifts) of the sources: the contribution of distant, small faint galaxies (with noisy shape measurements) to the measured lensing signal is smaller compared to brighter galaxies. The relative weight as a function of magnitude (see Figure 7 in Hoekstra et al. 2002a), is used to derive the "effective" redshift distribution. It turns out that this weighting scheme changes the redshift distribution only slightly. We refer to Hoekstra et al. (2000; 2002a) for a more detailed discussion of the photometric redshift distribution used here (also see Van Waerbeke et al. 2002).

It is expected that our knowledge of the redshift distribution of galaxies brighter than $R_C = 24$ will improve significantly in the near future. The current distribution is based on a relatively small sample of galaxies, and hence the data allow for a (small) range in redshift distributions.

To allow for this uncertainty in the redshift distribution we marginalize our model predictions over the redshift distribution allowed by the measurements of Fernández-Soto et al. (1999). To do so, we parametrize the redshift distribution using

$$p_b(z) = \frac{\beta}{z_s \Gamma\left(\frac{1+\alpha}{\beta}\right)} \left(\frac{z}{z_s}\right)^{\alpha} \exp\left[-\left(\frac{z}{z_s}\right)^{\beta}\right]. \qquad (15)$$

We fit this distribution to the observed "effective" redshift distribution, fixing $\alpha = 4.7$ and $\beta = 1.7$, which yields a best fit value of $z_s = 0.302$. We compute models for $z_s \in [0.274, 0.337]$, which correspond to the $\pm 3\sigma$ range

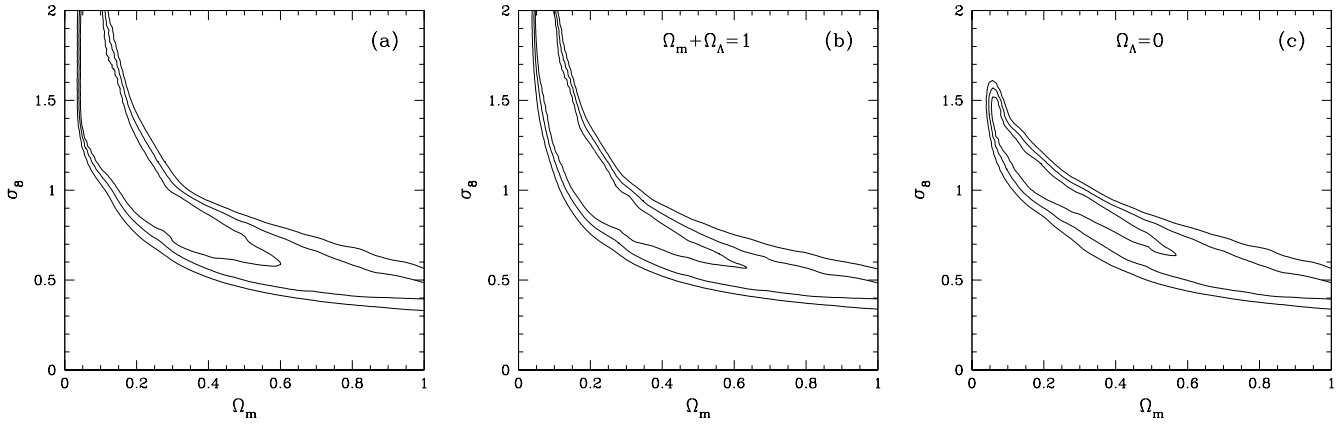

FIG. 3.— Contraints on Ω_m and σ_8 from RCS data only. The likelihood contours have been derived by comparing the measurements to CDM models with $n = 1$. We have marginalized the models over Γ and the z_s (for which we assumed a flat prior). The contours indicate the 68.3%, 95.4%, and 99.7% confidence limits on two paramaters jointly. Panel (a) shows the results marginalized over Ω_Λ; (b) gives the constraints for a flat cosmology (as suggested by the recent CMB results); (c) the results for an open ($\Omega_\Lambda = 0$) cosmology.

indicated by χ^2 of the fit to the photometric redshift distribution. For this choice of parameters the range in mean source redshift is $\langle z\rangle = 0.54 - 0.66$.

4.2. *Parameter estimation*

In this section we briefly discuss how we obtain constraints on some of the cosmological parameters. The relevant parameters for the analysis presented here are the mass density Ω_m, the normalization of the power spectrum σ_8 and the shape parameter Γ (note that $\Gamma \sim \Omega_m h$ in CDM cosmologies).

We also consider Ω_Λ, although the RCS results are not expected to provide strong constraints on Ω_Λ, because lensing is not sensitive to this parameter. However, the combination of the RCS measurements with the VIRMOS-DESCART results (Van Waerbeke et al. 2001a; 2002) can provide stronger constraints, because the two surveys probe the matter power spectrum at different redshifts. Hence, such a combined analysis enables a measurement of the growth of structure, and as a result it can break some of the degeneracies limiting our analysis. Furthermore, we can impose priors on some of the parameters based on external measurements, such as the CMB or redshift surveys.

We compute model predictions on a grid, which are subsequently compared to the data. We have limited the model parameters to a realistic range. We consider $\Omega \in [0, 1]$, $\Omega_\Lambda \in [0, 1]$, $\sigma_8 \in [0, 2]$, and $\Gamma \in [0.05, 0.5]$. As mentioned above, we use $z_s \in [0.274, 0.337]$ to account for the uncertainty in the source redshift distribution.

The measurements of $\langle M_{\rm ap}^2\rangle$ at different scales are slightly correlated. In order to compare the measurements to the models we have to compute the covariance matrix $\mathbf{C}$ which is given by

$$C_{ij} = \langle (d_i - \mu_i)^T (d_j - \mu_j)\rangle, \qquad (16)$$

where d_i is the measurement at scale θ_i, and μ_i is the "true" value for this scale (for which we take ensemble averaged value from the data). We compute the covariance matrix from the variance in the measurements for the 13 different patches, and hence it includes the cosmic variance. For a given model, we can compute the χ^2 (log-likelihood)

$$\chi^2 = (d_i - m_i)\mathbf{C}^{-1}(d_i - m_i)^T, \qquad (17)$$

which can be used to derive the likelihood for each set of parameters. From the measured χ^2 values it is straightforward to calculate the confidence contours.

4.3. *Joint constraints on Ω_m and σ_8*

We first consider the constraints we can derive on the combination of Ω_m and σ_8 from the RCS data alone. Without external priors these two cosmological parameters are degenerate. However, studies of cluster abundances give similar constraints, and it is therefore useful to compare the lensing results to the latter, popular technique.

Figure 3 shows the joint constraints on Ω_m and σ_8. We have marginalized over Γ and z_s, for which we assumed flat priors (i.e., all values have equal likelihood), which is rather conservative. Panel a shows the most general result, where we marginalize over Ω_Λ as well. For this choice of priors, we obtain $\sigma_8 = 0.45^{+0.09}_{-0.12}\Omega_m^{-0.55}$ (95% confidence).

The current CMB measurements favor a flat cosmology (e.g., de Bernardis et al. 2000; Jaffe et al. 2001; Netterfield et al. 2001; Pryke et al. 2002; Stompor et al. 2001), and the results for these models are presented in panel b. For reference we also show the results for an open ($\Omega_\Lambda = 0$) universe.

The current constraints on Ω_m and σ_8 in Figure 3 are degenerate from lensing alone. The degeneracies can be broken by measuring the cosmic shear signal in both the linear and the non-linear regime (Jain & Seljak, 1997). However, the accuracy of our measurements at small scales (non-linear regime) is limited by the observed "B"-mode in the data. Hence, due to the increased uncertainties on small scales, we cannot break the degeneracy.

However, if the "B"-mode is caused by intrinsic alignments of galaxies, forthcoming multi-color data can be used to derive crude photometric redshifts, and we might be able to remove the contribution of intrinsic alignments

by correlating the shapes of galaxies at different redshifts. In addition, the planned CFHT Legacy Survey, which is a 170 deg^2 deep, multi-color survey will allow us to measure the cosmic shear signal with unprecedented accuracy, and these data will allow a determination of Γ, σ_8, Ω_m and Ω_Λ from the shear two-point functions alone.

We also note that in order to break the degeneracies, and infer the correct values for the various cosmological parameters, the prescription for the evolution of the non-linear power spectrum needs to be improved. Van Waerbeke et al. (2001b, 2002) showed that the non-linear predictions fail for some cosmologies. The current prescription (Peacock & Dodds 1996) is not accurate enough for the future measurements.

Fortunately, cosmological parameters can be estimated through a wide range of techniques, such as the fluctuations in the CMB and galaxy redshift surveys. We can use the most recent results as priors to obtain tighter constraints.

In Figure 4 we show the constraints on Ω_m and σ_8, when we use Gaussian priors for the source redshift distribution z_s, Γ as determined from the 2dF galaxy redshift survey (Peacock et al. 2001; Efstathiou et al. 2001), and $\Omega_{\rm tot} = \Omega_m + \Omega_\Lambda$ from the Boomerang CMB measurements (Netterfield et al. 2001). The contours have tightened considerably, and the data favor a low value for Ω_m. For this choice of priors, we find $\sigma_8 = (0.46^{+0.05}_{-0.07})\Omega_m^{-0.52}$ (95% confidence).

We have also investigated whether the RCS data can be used to constrain Γ. Using our set of Gaussian priors, we find that we can only place a lower bound on Γ. We find a 95% confidence lower limit of $\Gamma > 0.1 + 0.16\Omega_m$.

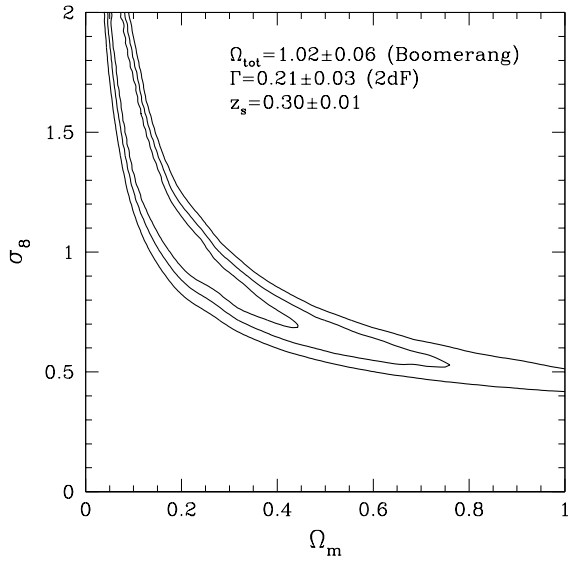

FIG. 4.— Contraints on Ω_m and σ_8 using Gaussian priors on Γ, $\Omega_{\rm tot} = \Omega_m + \Omega_\Lambda$, and the source redshift distribution z_s (which gives $\langle z \rangle = 0.59 \pm 0.02$). The likelihood contours have been derived by comparing the measurements to CDM models with $n_s = 1$. For Γ we used the constraints from the 2dF survey $\Gamma = 0.21 \pm 0.03$ (Peacock et al. 2001; Efstathiou et al. 2001), and for $\Omega_{\rm tot}$ we used the Boomerang constraints $\Omega_{\rm tot} = 1.02 \pm 0.06$ (Netterfield et al. 2001). The contours indicate the 68.3%, 95.4%, and 99.7% confidence limits on two paramaters jointly.

σ_8	priors
$0.88^{+0.04}_{-0.16}$	flat prior on z_s
$0.91^{+0.05}_{-0.12}$	flat prior on z_s, $\Omega_m + \Omega_\Lambda = 1$
$0.94^{+0.04}_{-0.06}$	flat prior on z_s, $\Omega_\Lambda = 0$
$0.86^{+0.04}_{-0.05}$	Gaussian priors on z_s, Γ, and $\Omega_{\rm tot}$

TABLE 1
Values of σ_8 and 68% confidence intervals for different priors, assuming $\Omega_m = 0.3$.

(a)	Cosmic shear survey	σ_8
	RCS	$0.86^{+0.04}_{-0.05}$
	Bacon et al. (2002)	$0.97^{+0.10}_{-0.09}$
	Refregier et al. (2002)	0.94 ± 0.14
	Van Waerbeke et al. (2002)	0.98 ± 0.06
(b)	Cluster abundance	σ_8
	Eke, Cole & Frenk (1996)	0.93 ± 0.07
	Carlberg et al. (1997)	0.82 ± 0.03
	Bahcall & Fan (1998)	$1.18^{+0.24}_{-0.22}$
	Pen (1998)	1.00 ± 0.09
	Borgani et al. (2001)	$0.72^{+0.07}_{-0.05}$
	Pierpaoli et al. (2001)	$1.02^{+0.07}_{-0.08}$
	Reiprich & Böhringer (2001)	$0.68^{+0.08}_{-0.06}$
	Seljak et al. (2001)	0.75 ± 0.06
	Viana et al. (2001)	0.61 ± 0.05

TABLE 2
(a) Values of σ_8 and 68% confidence intervals as derived from 4 independent cosmic shear measurements (adopting $\Omega_m = 0.3$, $\Omega_\Lambda = 0.7$, and $\Gamma = 0.21$; (b) determinations of σ_8 using cluster abundances.

For comparison to other work, we list the 68% confidence limits on σ_8 for $\Omega_m = 0.3$ for the different priors from our work in Table 1. It is also interesting to compare our results to other measurements. In Table 2a we list our measurements with the most recent measurements of σ_8 from weak lensing by large scale structure. The agreement between the four independent results is remarkable, in particular given the fact that the measurements are based on a wide variety of data sets, using different telescopes, filters, and depths. We can compute the ensemble averaged value of σ_8 from weak lensing, for which we find a value of 0.92 ± 0.03.

We note that the value of σ_8 determined from the RCS data is essentially constrained by the measurements at scales larger than 10 arcminutes, where the "B"-mode is negligible. The result from Van Waerbeke et al. (2002) might be biased high, because of their large scale "B"-mode. Both Bacon et al. (2002) and Refregier et al. (2002) do not separate their signal into "E" and "B"-modes, and therefore it might also include some residual systematics.

A widely used method to determine the normalization of the power spectrum uses the number density of rich clusters of galaxies (e.g., Borgani et al. 2001; Carlberg et al. 1997, Eke, Cole & Frenk 1998; Bahcall & Fan 1998; Pen 1998; Pierpaoli, Scott, & White 2001; Reiprich & Böhringer 2001; Seljak 2001; Viana, Nichol, & Liddle 2001). Such systems are rare, and as a result a very sen-

sitive probe of σ_8, provided one can determine their mass. Table 1b lists the results from 9 of these studies. The derived values for σ_8 from this technique range from values as low as 0.61 ± 0.05 (Viana et al. 2001) to values around unity (e.g., Bahcall & Fan 1998; Pen 1998; Pierpoali 2001). Unfortunately, it is currently unclear why some of the recent values from cluster abundances are this low. From Table 1b it is clear that there is a wide spread in values, whereas the statistical error bars are small. This points to underlying systematics, which complicate the determination of σ_8 from cluster abundances.

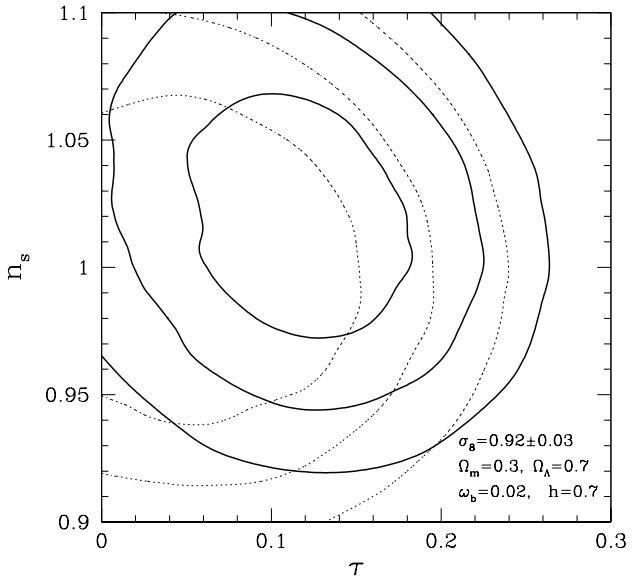

FIG. 5.— Joint constraints on the reionization optical depth τ and the scalar spectral index n_s from the combination of CMB results (compilation by Wang et al. 2001). We have marginalized over the value of σ_8, using a prior $\sigma_8 = 0.92 \pm 0.03$ as determined by the 4 most recent weak lensing measurements. The other cosmological parameters were fixed as indicated. The dotted contours indicate the constraints from RCS alone ($\sigma_8 = 0.86 \pm 0.05$). The contours correspond to the 68.3%, 95.4% and 99.7% confidence limits on the two parameters jointly.

4.4. *Limits on the reionization optical depth τ*

The measurements of the fluctuations in the CMB also give joint constraints on Ω_m and σ_8. Recently, several papers argue that the CMB results yield a low normalization for the matter power spectrum (e.g., Lahav et al. 2001; Melchiorri & Silk 2002), with values ranging from $0.73 - 0.8$.

However, the current CMB data give relatively weak constraints on σ_8, because the amplitude of the CMB power spectrum also depends on the reionization optical depth τ, and the scalar spectral index n_s. Once the universe is reionized, CMB photons can be Thomson scattered off of a free electron. As a result, the accousic peaks in the CMB power spectrum are suppressed. Although the effect is scale dependent (it does not affect the largest scales), it introduces a degeneracy between σ_8 and τ. The matter power spectrum probed by weak lensing is not affected, and hence, the combination of the CMB and weak lensing results, in principle, can constrain τ, and consequently the reionization redshift.

The CMB results are taken from the compilation by Wang, Tegmark, & Zaldarriaga (2001), which is a combination of many experiments, such as CBI (Padin et al. 2001), BOOMERANG (Netterfield et al. 2001), DASI (Halverson et al. 2002), and MAXIMA (Lee et al. 2001). We use these results to obtain joint constraints on τ, n_s and σ_8, adopting a baryon density $\omega_b = 0.02$, $h = 0.7$, $\Omega_m = 0.3$, and $\Omega_\Lambda = 0.7$. We use the CMBFAST code (Seljak & Zaldarriaga 1996) to compute the theoretical CMB power spectra, and use the window function and covariance matrix provided by Wang et al. (2001).

In Figure 5 we present the joint constraints on τ and n_s, where we marginalized over the value of σ_8, using the prior $\sigma_8 = 0.92 \pm 0.03$, as determined from weak lensing. The other cosmological parameters were fixed. The dotted contours correspond to the constraints derived from the RCS measurement of σ_8 alone. We stress that the results depend on the assumed priors (many cosmological parameters are fixed), and a full combined analysis of weak lensing and CMB data, marginalizing over all parameters, is required for definite results. However, the results presented here demonstrate that such a combined analysis can be fruitful.

For our choice of parameters, which are close to those favored by the vast amount of data currently available, we can derive constraints on n_s and τ. Marginalizing over τ, we find $n_s = 1.02^{+0.07}_{-0.06}$ with 95% confidence. For τ we obtain $\tau = 0.12 \pm 0.09$ (95% confidence, marginalized over n_s).

The reionization optical depth can be related to the redshift of reionization. To do so, we use (e.g., Hu 1995; Griffiths & Liddle 2001)

$$\tau(z) = 4.61 \times 10^{-2} \left(1 - \frac{Y_p}{2}\right) x_e \frac{\Omega_b h}{\Omega_m} \times \left[\sqrt{1 - \Omega_m + \Omega_m (1+z)^3} - 1\right], \qquad (18)$$

which is valid for flat cosmologies. Here $Y_p = 0.24$ is the primordial mass fraction in Helium, and x_e is the ionized fraction. For a fully reionized universe ($x_e = 1$) the resultant τ as a function of reionization redshift is presented in Figure 6. We have also indicated the 68% and 95% confidence limits on τ (hatched regions), based on our constraints on τ. This allows us to read off the reionization redshift $z_{\rm reion}$, for which we find $z_{\rm reion} = 14^{+7}_{-9}$ with 95% confidence.

5. CONCLUSIONS

We have analysed ~ 53 square degrees of R_C-band imaging data from the Red-Sequence Cluster Survey (RCS), and measured the excess correlations in the shapes of galaxies on scales out to one degree. To this end we use the aperture mass statistic, which allows a natural separation of the signal in a curl-free "E"-mode (which is expected from gravitational lensing) and a "B"-mode which provides an important measure of residual systematics and the contribution from intrinsic alignments.

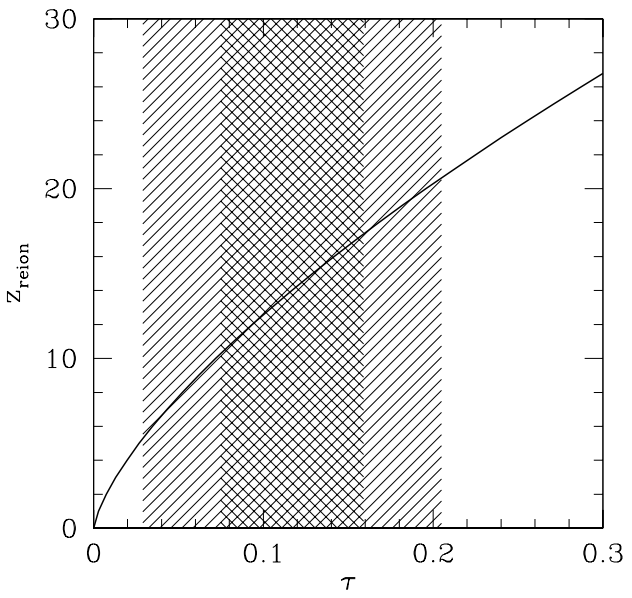

FIG. 6.— The reionization redshift as a function of optical depth τ as given by Eq. 18 (solid line). The hatched regions indicate the 68% and 95% confidence limits on τ. This corresponds to a reionization redshift of $z_{\rm reion} = 14^{+7}_{-9}$ (95% confidence).

For the lensing analysis we have selected a sample of galaxies with $20 < R_C < 24$. On scales larger than 10 arcminutes the "B"-mode vanishes, and therefore we are able to measure the cosmic shear signal with high accuracy on these scales. On smaller scales we find a small "B"-mode. We split the sample in bright ($20 < R_C < 22$) and faint ($22 < R_C < 24$) galaxies, and find a significant "B"-mode for the bright sample. These galaxies are large compared to the PSF, and therefore are not very sensitive to errors in the corrections for observational distortions. However, these galaxies probe only a relatively small range in redshift, and intrinsic alignments of galaxies are expected to be important. Intrinsic alignments can introduce a "B"-mode and we conclude that the observed signal is likely to be caused by this effect. A multi-color catalog, which is currently being created, will provide stronger constraints as it provides a better redshift discrimination of the galaxies.

The faint sample also shows a small "B"-mode, but it is smaller than the "E"-mode signal. It is not clear what is the cause of this signal, and hence the correction is uncertain. As a conservative approach we add the amplitude of the "B"-mode signal to the uncertainty in the measurement of the lensing signal. These measurements are then used to derive constraints on cosmological parameters.

The relevant cosmological parameters for the analysis presented here are the mass density Ω_m, the cosmological constant Ω_Λ, the normalization of the power spectrum σ_8 and the shape parameter Γ (note that $\Gamma \sim \Omega_m h$ in CDM cosmologies). To relate the model predictions to the data we use photometric redshift distributions for our sample of source galaxies ($22 < R_C < 24$), and marginalize over the uncertainty in the source redshifts.

We investigated whether the RCS data can be used to constrain Γ. Using Gaussian priors for Γ (from 2dF) and $\Omega_m + \Omega_\Lambda$ (from CMB), and the redshift distribution, we find that we can only place a lower bound on Γ for which we find $\Gamma > 0.1 + 0.16\Omega_m$ (95% confidence).

We derive joint constraints on Ω_m and σ_8, by marginalizing over Γ, Ω_Λ and the source redshift distribution, using different priors. Marginalizing over Γ and Ω_Λ, and using a flat prior for the source redshift distribution, yields a conservative constraint of $\sigma_8 = 0.45^{+0.09}_{-0.12}\Omega_m^{-0.50}$ (95% confidence). A better constraint is derived when we use the Gaussian priors, which yields $\sigma_8 = 0.46^{+0.05}_{-0.07}\Omega_m^{-0.52}$ (95% confidence).

Comparison of the RCS results with three other recent cosmic shear measurements shows excellent agreement (Bacon et al. 2002; Refregier et al. 2002; van Waerbeke et al. 2002), and we find an ensemble averaged value of $\sigma_8 = 0.92 \pm 0.03$ (68% confidence). The value of σ_8 determined from the RCS data appears to be free of systematics. It is not clear, however, whether the results from the other surveys are biased high as a result of residual systematics. Some recent studies (Reiprich et al. 2001; Seljak et al. 2001; Viana et al. 2001) of the abundance of rich clusters suggest low values for σ_8, which disagree with the lensing results with high confidence. The reason for this discrepancy is currently unclear.

The weak lensing results are also in good agreement with CMB measurements, when we allow the reionization optical depth τ and the spectral index n_s to vary. We have presented a simple demonstration of how the weak lensing results can be used as a prior for the parameter estimation from CMB measurement. We found that we can derive constraints on τ and n_s (fixing $\Omega_m = 0.3$, $\Omega_\Lambda = 0.7$, $\omega_b = 0.02$, and $h = 0.7$). Doing so, we obtain $n_s = 1.02^{+0.07}_{-0.06}$ and $\tau = 0.12 \pm 0.09$, both with 95% confidence. We can relate the value of τ to the reionization redshift $z_{\rm reion}$ for which we find $z_{\rm reion} = 14^{+7}_{-9}$ with 95% confidence. We stress, however, that the results depend on the assumed priors, and that a full combined analysis of weak lensing and CMB data, marginalizing over all parameters, is required for definite results. Our preliminary results, however, are not inconsistent with the latest observations of quasars at $z \sim 6$, which indicate that the universe may be just exiting the reionization epoch at that time (Barkana 2002; Becker et al. 2001; Djorgovski et al. 2001; Fan et al. 2002).

REFERENCES

Bacon, D., Refregier, A., & Ellis, R.S. 2000, MNRAS, 318, 625
Bacon, D., Massey, R., Refregier, A., & Ellis, R. 2002, MNRAS, submitted, astro-ph/0203134
Bahcall, N.A. & Fan, X. 1998, ApJ, 504, 1
Barkana, R. 2002, New Astronomy, 7, 85
Bartelmann, M., & Schneider, P. 2001, Physics Reports, 340, 291
Becker, R.H., et al. 2001, AJ, 122, 2850
Borgani, S., et al. 2001, ApJ, 561, 13
Carlberg, R. G., Morris, S. L., Yee, H. K. C., Ellingson, E. 1997, ApJ, 479, L19
Catelan, P., Kamionkowski, M., & Blandford, R.D. 2001, MNRAS, 320, L7
Cohen, J.G., Hogg, D.W., Blandford, R.G., Cowie, L.L., Hu, E., Songaila, A., Shopbell, P., & Richberg, K. 2000, ApJ, 538, 29
Crittenden, R.G., Natarajan, P., Pen, U.-L., & Theuns, T. 2001, ApJ, 559, 552

Crittenden, R.G., Natarajan, P., Pen, U.-L., & Theuns, T. 2002, ApJ, in press, astro-ph/0012336
de Bernardis, P., et al. 2000, Nature, 404, 955
Djorgovski, S.G., Castro, S., Stern, D., & Mahabal, A.A. 2001, ApJ, 560, L5
Efstathiou G., et al. 2001, MNRAS, submitted, astro-ph/0109152
Eke, V.R., Cole, S., Frenk, C.S. 1996, MNRAS, 282, 263
Gladders, M.D., & Yee, H.K.C. 2000, to appear in "The New Era of Wide-Field Astronomy", astro-ph/0011073
Griffiths, L., & Liddle, A. 2001, MNRAS, 324, 769
Fan, X., Narayanan, V.K., Strauss, M.A., White, R.L., Becker, R.H, Pentericci, L., & Rix, H.-W. 2002, AJ, 123, 1247
Fernández-Soto, A., Lanzetta, K.M., & Yahil, A. 1999, ApJ, 513, 34
Halverson, N.W., et al. 2002, ApJ, 568, 38
Heavens, A., Refregier, A., & Heymans, C. 2000, MNRAS, 319, 649
Hoekstra, H., Franx, M., Kuijken, K. 2000, ApJ, 532, 88
Hoekstra, H. 2001, A&A, 370, 743
Hoekstra, H., Yee, H.K.C, Gladders, M.D. 2001, ApJ, 558, L11
Hoekstra, H., Yee, H.K.C., Gladders, M.D., Barrientos, L.F., Hall, P.B., & Infante, L. 2002a, ApJ, in press
Hoekstra, H., van Waerbeke, L., Gladders, M.D., Mellier, Y., & Yee, H.K.C. 2002b, ApJ, submitted
Hu, W.T. 1995, PhD thesis, UC Berkeley
Jaffe, A.H., et al. 2001, Phys. Rev. Lett. 86, 3475
Jain, B., & Seljak, U. 1997, ApJ, 484, 560
Kaiser, N., Squires, G., Fahlman, G. G., & Woods, D. 1994, in "Clusters of Galaxies", eds. Durret, Mazure, Tran Thanh Van
Kaiser, N., Wilson, G., & Luppino, G.A. 2000, ApJL, submitted, astro-ph/0003338
Lahav, O. et al. 2001, MNRAS, submitted, astro-ph/0112162
Lee, A.T., et al. 2001, ApJ, 561, L1
Mackey, J., White, M., & Kamionkowski, M. 2001, MNRAS, submitted, astro-ph/0106364
Maoli, R., Van Waerbeke, L., Mellier, Y., Schneider, P. Jain, B., Bernardeau, F., Erben, T. & Fort, B. 2001, A&A, 368, 766
Melchiorri, A. & Silk, J. 2002, astro-ph/0203200
Netterfield, C.B. et al. 2001, astro-ph/0104460
Padin, S., et al. 2001, ApJ, 549, L1
Peacock, J.A., & Dodds, S.J. 1996, MNRAS, 780, L19
Peacock, J.A. et al. 2001, Nature, 410, 169
Pen, U.-L. 1998, ApJ, 504, 60
Pen, U.-L., van Waerbeke, L., Mellier, Y. 2002, ApJ, 567, 31
Percival, W.J. et al. 2001, MNRAS, 327, 1297
Pierpaoli, E., Scott, D., & White, M. 2001, MNRAS, 325, 77
Pryke, C., Halverson, N.W., Leitch, E.M., Kovac, J., Carlstrom, J.E., Holzapfel, W.L., & Dragovan, M. 2002, ApJ, 568, 46
Refregier, A., Rhodes, J., & Groth, E.J. 2002, ApJL, submitted, astro-ph/0203131
Reiprich, T.H. & Böhringer, H. 2001, astro-ph/0111285
Schneider, P., van Waerbeke, L., Jain, B., & Kruse, G. 1998, MNRAS, 296, 873
Schneider, P., van Waerbeke, L. & Mellier Y. 2002, A&A, submitted, astro-ph/0112441
Seljak, U. 2001, MNRAS, sumbitted, astro-ph/0111362
Seljak, U. & Zaldarriaga, M. 1996, ApJ, 469, 437
Stompor, R., et al. 2001, ApJ, 561, L7
Strauss, M.S. & Willick, J.A. 1995, Phys. Rep., 261, 271
van Waerbeke, L., et al. 2000, A&A, 358, 30
van Waerbeke, L., et al. 2001a, A& A, 374, 757
van Waerbeke, L., Hamana, T., Scoccimarro, R., Colombi, S., Bernardeau, F. 2001b, MNRAS, 322, 918
van Waerbeke, L., Mellier, Y., Pello, R., Pen, U.-L., McCracken, H.J., Jain, B. 2002, A&A, submitted, astro-ph/0202503
Viana, P.T.P., Nichol, R.C., Liddle, A.R. 2001, ApJL, submitted, astro-ph/0111394
Wang, X., Tegmark, M., Zaldarriaga, M. 2001, astro-ph/0105091, Phys. Rev. D, in press
Wittman, D.M., Tyson, J.A., Kirkman, D., Dell'Antonio, I., & Bernstein, G. 2000, Nature, 405, 143
Yee, H.K.C., & Gladders, M.D. 2001, in "AMiBA 2001: High-z Clusters, Missing Baryons, and CMB Polarization", ASP Conference Series, Eds. L.-W. Chen et al., astro-ph/0111431